Influence of salt contamination on consolidation of slaked lime mortar by ammonium phosphate and nanolimes

INFLUENCE OF SALT CONTAMINATION ON CONSOLIDATION OF SLAKED LIME MORTAR BY AMMONIUM PHOSPHATE AND NANOLIMES

Greta Ugolotti[1], Giulia Masi[1], Elisa Boanini[2], Enrico Sassoni[1,*]

[1] Dept. Civil, Chemical, Environmental & Materials Engineering (DICAM)

University of Bologna - Via Terracini 28, 40131, Bologna, Italy

[2] Dept. Chemistry "Giacomo Ciamician", University of Bologna - Via Selmi 2, 40126, Bologna, Italy

* Corresponding author: enrico.sassoni2@unibo.it

ABSTRACT

This study aimed at evaluating the influence of salt contamination on the performance of two consolidants (diammonium hydrogen phosphate, DAP, and nanolimes, NL), applied onto slaked lime-based mortars contaminated with sodium sulfate before and/or after consolidation. The strengthening ability of the two treatments was assessed in terms of dynamic elastic modulus and compressive strength by double punch test, while the alterations in the pore system were evaluated by MIP and the features of the new consolidating phases were assessed by XRD and FEG-SEM. To test the durability of the consolidated mortars, salt weathering cycles were performed by alternating immersion into a 14 wt% aqueous solution of $Na_2SO_4 \cdot 10H_2O$ and drying in oven, as recommended by the European Standard EN 12370. The effects of the salt weathering cycles were assessed by measuring the changes in weight and dynamic elastic modulus after each cycle and the residual compressive strength after 10 cycles and desalination. The results of the study show that, right after the consolidant application, with or without salts initially present in the mortar, the strengthening ability of DAP was higher than that of NL. The DAP treatment induced formation of carbonate hydroxyapatite, as assessed by XRD, and notably the initial presence of salt inside the mortar pores did not negatively affect the outcome of the treatment. However, the formation of carbonate hydroxyapatite was responsible for a shift of the pore size distribution towards smaller pores, which may increase the stress generated by salt crystallization. When the consolidated mortar specimens were subjected to salt weathering cycles, both consolidants provided some benefit against salt weathering, but the high aggressiveness of the salt weathering test might have reduced the performance of the consolidants.

KEYWORDS

Salt weathering; Salt contamination; Sodium sulfate; Na_2SO_4; Hydroxyapatite; Carbonate hydroxyapatite; Calcium phosphate; Nanoconsolidants; Inorganic consolidants; Desalination

1. INTRODUCTION

Salt crystallization is one of the major causes of deterioration of porous building materials, such as stones, mortars and plasters [1,2]. Saline solutions can be brought into porous materials by various mechanisms, especially capillary rise from the ground. Depending on the evaporation conditions and the pore size distribution of the substrate (possibly composed of various layers with different porosity, like in the case of frescoes and wall paintings), salt crystallization may occur on the surface (efflorescence) or in depth in the material (subflorescence) [3]. While efflorescence is mostly unaesthetic, subflorescence is particularly dangerous for the conservation of porous substrates. Indeed, when the pressure exerted by the growing crystals exceeds the tensile strength of the material, damage occurs in the form of cracking, powdering and material loss.

To prevent and limit damage caused by salt crystallization, some innovative strategies have been recently proposed, such as crystallization inhibitors [4] and treatments to modify the salt crystallization behavior [5]. However, the standard practice to tackle salt damage is usually to first remove salts already present inside the substrate and then to apply a consolidating treatment to increase the mechanical properties of the substrate.

Salt removal can be performed by applying a poultice of cellulose pulp or clays soaked with deionized water [6]. However, depending on the deterioration conditions of the substrate, poultice application is not always feasible and, in extreme cases, pre-consolidation of the substrate is necessary before salt removal can be attempted. Pre-consolidation requires the selection of a suitable consolidant, in terms of solvent, active principle and alterations in the substrate wettability and pore size distribution. As a result, consolidating treatments are often applied onto porous substrates that still contain a certain amount of soluble salts, because (i) pre-consolidation is necessary before salt removal, (ii) salt extraction by poulticing has resulted in incomplete salt removal, (iii) a continuous source of saline solution is present (e.g. rising damp from the ground) and/or (iv) constraints during the conservation work (e.g. time and cost) make salt removal by poulticing not feasible.

The presence of salts inside the substrate when a consolidant is applied is actually a fundamental aspect, because the chemical reactions responsible for the hardening of the consolidant may be altered and the bonding between the consolidant and the substrate may be compromised, resulting in the failure of the consolidating work [7]. Even though consolidant application onto salt-laden substrates is quite frequent in the conservation practice, only a limited number of studies has systematically investigated the behavior of the most diffused inorganic consolidants when applied onto salt-contaminated substrates:

- Ethyl silicate: in some studies the consolidating ability has been found to be not dramatically decreased in the presence of salts [8,9], but this trend is not univocal [8-11]. In fact, the alterations in pore size distribution caused by ethyl silicate may increase the crystallization

pressure exerted by salts, resulting in decreased salt resistance of the treated substrate [8,12,13].

- Nanolimes: also in this case mixed results have been reported about the treatment effectiveness on salt-laden substrates [8,14], again because of the increase in crystallization pressure caused by the modification in pore size distribution after treatment [14].
- Ammonium oxalate: encouraging results have been found when the treatment was applied onto salt-laden substrates [15-17], although the treatment tends to form a superficial coating, so that a limited ability to consolidate the substrate in depth has been highlighted [18].
- Ammonium phosphate: alongside a general increase in salt resistance after consolidation of salt-free substrates [12,13,19], encouraging results have been reported also when the treatment was applied onto salt-contaminated stones [9,20].

In the light of the findings briefly summarized above, the present study aims at systematically investigating the effects of salt presence inside the pores of slaked lime-based mortar when consolidated with ammonium phosphate or nanolimes. Slaked lime-based mortars were selected as reference substrate as they have been used in the past for both structural and decorative functions, so that innovative methods for assessment and improvement of their mechanical properties [21] and durability [22] are frequently necessary.

The ammonium phosphate treatment consists in the application of an aqueous solution of diammonium hydrogen phosphate (DAP), to induce formation of new calcium phosphates as the reaction product between calcium ions from the substrate and phosphate ions from the DAP solution [23]. This treatment was selected for the present study considering that, following the promising results obtained for stone consolidation [23] and protection [24,25], recent studies have shown its effectiveness for consolidation of mortars based on slaked lime, natural hydraulic lime and cement [26-29]. In the case of DAP, the issue of salt presence when the treatment is applied is particularly important, considering that the new calcium phosphates formed after treatment are easily subject to various ion substitutions, resulting in significantly different properties (e.g. solubility) [30,31]. In case calcium phosphate phases with high solubility were formed, then their beneficial effect could be rapidly lost as they could be solubilized by rising damp or rainfall, hence it is essential to make sure that only calcium phosphates with very low solubility be formed.

The treatment based on nanolimes (NL) consists in the application of an alcoholic dispersion of $Ca(OH)_2$ nanoparticles, which transform into $CaCO_3$ upon reaction with atmospheric CO_2 [32]. This treatment was selected for the present study considering that nanolimes are frequently used in the practice of plaster, frescoes and wall paintings consolidation [33].

In the specific case of lime mortars, previous comparative studies have shown that the DAP treatment is able to provide greater mechanical strengthening than the NL treatment, with the additional advantage that a much shorter time is needed (24 hours instead of 4 weeks) [28,29]. In

addition, the DAP treatment has also shown higher durability to freezing-thawing cycles than the NL treatment [28,29], so the present study also aimed at extending the literature on the durability of mortars consolidated by these two treatments. In the present study, the compatibility of the two treatments was not specifically assessed, considering that the cited previous study showed that both DAP and NL can be considered as fairly compatible, in terms of alterations in color, porosity and water absorption [29].

To evaluate the effectiveness and the durability of the two consolidating treatments in conditions as realistic as possible, preliminary salt contamination was also performed on part of the mortar specimens. Overall, four conditions were considered (Figure 1): (i) non-contaminated specimens; (ii) pre-contaminated specimens; (iii) non-contaminated specimens, then subjected to salt crystallization cycles; (iv) pre-contaminated specimens, then subjected to further salt crystallization cycles. For each condition, untreated references (UT) were compared to specimens consolidated with ammonium phosphate (DAP) or nanolimes (NL).

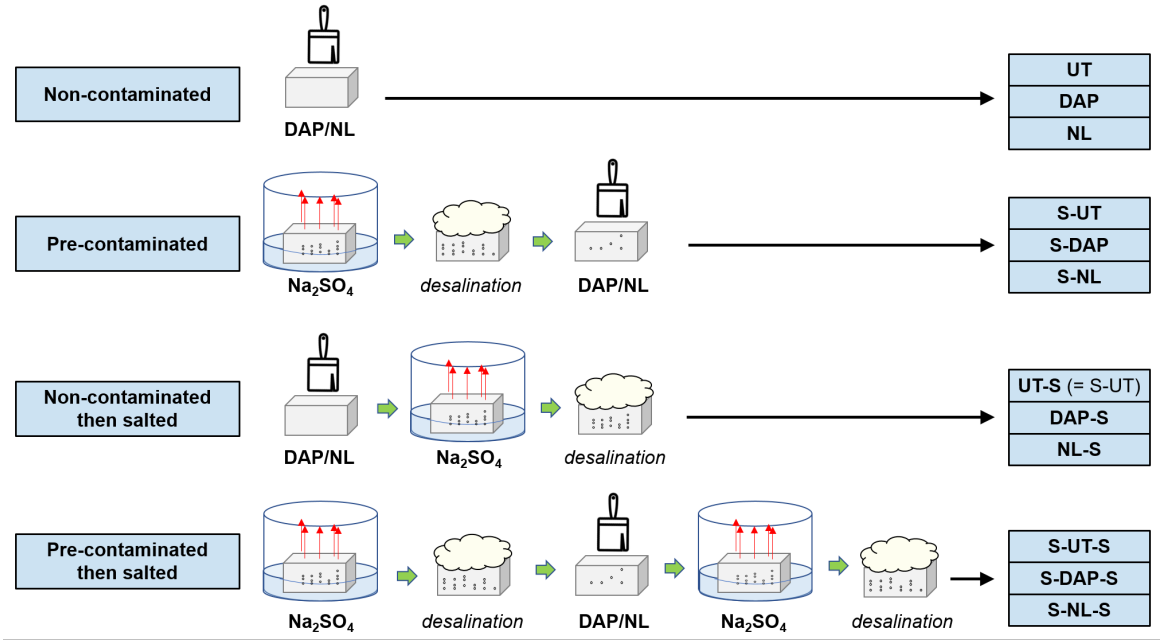

Figure 1. Schematic illustration of the four conditions examined in the study: (i) Non-contaminated specimens; (ii) Pre-contaminated specimens ("S-" prefix); (iii) Non-contaminated specimens, then salted ("-S" suffix); (iv) Pre-contaminated specimens, then salted ("S-" prefix and "-S" suffix). Treatment conditions: UT = untreated reference; DAP = treated with ammonium phosphate; NL = treated with nanolimes. The "S-UT" condition is the same as the "UT-S", as no consolidation treatment is involved.

2. MATERIALS AND METHODS

3.1. Mortar samples

The mortar preparation was designed to produce specimens with composition similar to historic mortars, using slaked lime by Colacem, Italy (CL 70-S according to EN 459-1:2015) and calcareous

sand (having a $CaCO_3$ content of 95 ± 1.5 wt% and maximum particle size of 4 mm). A water-to-binder ratio of 1:1 v/v (corresponding to 0.45 w/w) and a binder-to-aggregate ratio of 1:2 v/v (corresponding to 0.41 w/w) were adopted. This binder-to-aggregate ratio was selected from the range reported in the literature for wall paintings (1:3 to 1:2, depending on the layer [34]), as this ratio was often used for the most superficial layers ("*Intonaco*" and "*Intonachino*"), which are the ones over which the consolidants would be applied in the case of wall painting consolidation.

Prismatic specimens (3×2×16 cm^3) were prepared using purposely-built molds, where the fresh mortar, prepared in a Hobart mixer, was poured. After manual compaction and leveling, the mold was immediately removed and the prisms were left to cure in a climatic chamber (RH = 90 ± 2% and T = 21 ± 2 °C) for 4 months, followed by additional curing in laboratory conditions (RH = 50 ± 5% and T = 21 ± 2 °C) for 3 months. The initial curing at high RH was aimed at favoring carbonation, considering that carbonation of $Ca(OH)_2$ nanoparticles has been reported to be accelerated at RH increasing from 33% up to 95% [32].

After curing for a total of 7 months, the original prisms were hand sawn to obtain 3×3×2 cm^3 specimens. To compensate for the possible variability in the properties of the different prisms, from each prism 3 samples were obtained and used one for each of the 3 different conditions (UT, DAP, NL). At least 3 replicates were used for each condition.

3.2. Sample pre-contamination

As illustrated in Figure 1, half of the specimens ("S-" prefix) was preliminarily exposed to salt solutions before consolidant application. Pre-contamination was obtained by partially immersing samples in a 14 wt% aqueous solution of $Na_2SO_4 \cdot 10H_2O$ (Sigma Aldrich, reagent grade). Sodium sulfate was selected considering that this salt is known to be one of the most damaging salts affecting building materials [35]. The adopted concentration (corresponding to saturation at room temperature) was used following the recommendation in the European Standard EN 12370 [36]. It is noteworthy that this standard has been criticized to be too aggressive and thus not fully representative of salt weathering occurring in the field, so the scientific community is currently working to develop a more reliable accelerated test [35]. However, in the lack of a commonly accepted alternative procedure when the study was performed, the conditions recommended in the European standard were adopted for the study, the only exception being that samples were partially immersed in the salt solution (as recommended in the scientific literature [37]) instead of being totally immersed (as recommended in the European Standard [36]). The samples were partially immersed by placing them in a beaker, with the 3x3 cm^2 face in contact with the container, then pouring the salt solution until reaching half of the 2 cm height. The container was then sealed with Parafilm® to prevent evaporation. After partial immersion for 2 hours (sufficient for full saturation), the samples

were extracted from the salt solution and dried in an oven at 40 °C for 20 hours. After cooling down to room temperature for 2 hours, variations in sample weight and dynamic elastic modulus (E_d) were registered, following the procedure described in § 3.5.

The salt crystallization cycle (2 h partial immersion, 20 h drying, 2 h cooling) was repeated until a total of 6 cycles was performed. This number of cycles was selected based on preliminary tests, which showed that in this was a significant but not excessive level of damage (in terms of weight loss and decrease in E_d) could be induced in the mortar samples.

Before consolidant application, the salt-contaminated samples were subjected to salt extraction by poulticing, to reproduce the conditions that would be experienced in the field when cleaning precedes consolidation. Desalination was performed by applying a poultice of cellulose pulp and deionized water (1:4 w/w ratio) all around the samples (putting a sheet of Japanese paper between the samples and the poultice, to avoid sticking). The samples with the poultice were wrapped in a plastic film for 24 hours, to avoid evaporation, then the film was removed and the poultice was left to dry at room temperature for 72 hours, while still in contact with the samples. The amount of sulfate remaining in the samples was determined by ion chromatography, as described in § 3.5. Two desalination treatments were applied, until the sulfate content decreased below the value (0.25 wt%) that has been pointed out in the literature as the critical limit over which salt extraction by poulticing is necessary [38]. After the second desalination, the variation in pore size distribution was assessed by mercury intrusion porosimetry (MIP), as described in § 3.5.

3.3. Consolidating treatments

For the DAP treatment, diammonium hydrogen phosphate ($(NH_4)_2HPO_4$, DAP), kindly supplied by CTS s.r.l. (Italy), and deionized water were used. Based on previous studies [39,40], an aqueous solution of 3 M DAP (corresponding to 396 g/L of DAP) was used, as this formulation allows achieving strong mechanical consolidation even in highly deteriorated substrates. The DAP solution was applied by brushing onto one of the 3x3 cm^2 faces until apparent refusal, intended as the condition when the treated surface remains wet for more than 1 minute after the consolidant application. Treatment until apparent refusal was selected, considering that this condition is recommended in the technical data sheet of the alternative consolidant (NL), so that the comparison between the two products could be performed in the same conditions. Given the high porosity of the mortar samples, apparent refusal occurred after brushing for 40 times. At the end of the brush application, the specimens were wrapped in a plastic film for 24 h to allow for reaction and to prevent evaporation. Then, the samples were unwrapped, rinsed with deionized water and left to dry at room temperature until constant weight. Afterwards, a limewater poultice was applied, to remove unreacted DAP that may remain in the substrate when highly concentrated solutions are used

[39,40]. A poultice was prepared using cellulose pulp and a saturated solution of $Ca(OH)_2$ (i.e. limewater), using a 1:4 w/w ratio. The poultice was applied onto the DAP-treated samples (again inserting a sheet of Japanese paper), then the samples were wrapped in a plastic film for 24 hours. Afterwards, the film was removed and the poultice was left to dry at room temperature until constant weight, so that unreacted DAP could be transported into the poultice during drying [40]. The samples were finally rinsed with water, then dried at room temperature and stored in the same conditions as the NL samples until testing.

For the NL treatment, the commercial product Nanorestore Plus Propanol 5, kindly supplied by CTS S.r.l. (Italy), was used. The product was applied onto one of the 3×3 cm^2 faces until apparent refusal, as recommended in the product's technical data sheet, which was reached after 30 brush strokes. Following the recommendation in the technical data sheet, the product was applied through a sheet of Japanese paper, to avoid surface whitening. At the end of the application, a poultice of cellulose pulp and deionized water (1:4 w/w ratio) was applied over the treated surface (without removing the Japanese paper), as recommended by the manufacturer. After drying, the poultice was removed and the specimens were cured at RH = 90 ± 2% and T = 21 ± 2 °C for 1 month before testing, thus adopting the curing time recommended by the manufacturer.

Before testing, all the specimens were dried in an oven at 40 °C for 72 hours.

3.4. Resistance to salt weathering after consolidation

As illustrated in Figure 1, half of the samples ("-S" suffix) was subjected to further salt crystallization cycles after consolidation, to test the ability of the consolidating treatments to increase the resistance to salt weathering. In this phase, 10 salt crystallization cycles were performed, following the same procedure described in § 3.2. After each cycle, the change in the sample appearance was checked by visual inspection and the variations in weight and E_d were registered. After the 10^{th} cycle, the samples were desalinated twice by poulticing, as described in § 3.2. The effects of the salt crystallization cycles were then assessed as described in § 3.5.

3.5. Sample characterization

The changes in mortar cohesion after (i) preliminary contamination with salts, (ii) consolidation and (iii) salt crystallization cycles after consolidation, were monitored non-destructively by measuring the dynamic elastic modulus (E_d). E_d has been shown to be strongly correlated with porosity and mechanical properties in natural stones, especially marble [41,42], so it is frequently used also on mortars [26,27,43]. E_d was calculated using the formula $E_d = \rho \times UPV^2$, where ρ is the density and UPV is the ultrasonic pulse velocity, measured using a Pundit instrument with 55 kHz transducers.

To improve the contact between the transducers and the samples, a rubber couplant was used. The UPV and, hence, E_d were determined in two directions, perpendicular ($E_{d\perp}$) and parallel ($E_{d//}$) to the 3×3 cm^2 face of the samples, with the aim of taking into account: (i) any anisotropy that could be present in the manually compacted mortar samples; (ii) the effect of salt contamination, as the saline solution penetrated into the specimens through one 3×3 cm^2 face while evaporation took place through the opposite 3×3 cm^2 face, so that salt accumulation in this latter face is expected; (iii) the effect of consolidation, as a gradient in properties may occur starting from the treated surface (i.e. the 3×3 cm^2 face through which evaporation took place) [39]. Because the presence of salts inside pores and microcracks alters the E_d measurements (the ultrasonic pulse travels faster when voids are filled with salts), at the end of the salt weathering cycles the specimens were desalinated by poulticing as described in § 3.2 and the E_d measurement was repeated.

A further estimation of the damaging effect of salts and of the strengthening effect of the consolidants was obtained by measuring the mortar compressive strength by double punch test (DPT), performed after desalination. The mortar specimens were loaded in the center of the two 3×3 cm^2 faces by means of two circular steel plates with 20 mm diameter, according to the procedure originally proposed in [44]. The size of the platens was selected considering that a previous study has shown that a good estimation of the actual mortar compressive strength can be obtained when the diameter of the platens (in this case, 20 mm) equals the thickness of the mortar sample (in this case, 20 mm) [45]. Because the DPT is sensitive to the specimen surface roughness (as irregularities may lead to stress accumulation), the contact area was gently smoothened by using sandpaper.

The alterations in open porosity and pore size distribution owing to salt damage and to consolidation were evaluated by mercury intrusion porosimetry (MIP). MIP samples (~1 cm^3) were obtained from the specimens that had been subjected to desalination and DPT. They were analyzed using a Pascal 140 and 240 instrument (minimum pressure 0.0125 MPa, maximum pressure 200 MPa).

The surface morphology of one sample for each condition was observed using a field emission gun scanning electron microscope (FEG-SEM, Tescan Mira 3, WD = 10 mm, Voltage = 10 kV). The SEM samples were obtained from the specimens that were used for DPT, after desalination. Before SEM observation, the samples were made conductive by sputtering with aluminum.

In the case of the DAP treatment, the crystalline phase composition of the surface of the untreated reference samples (non-contaminated, “UT”, and pre-contaminated, “S-UT”) and of the DAP-treated samples (“DAP”, “S-DAP”, “DAP-S” and “S-DAP-S”) was analyzed by powder X-ray diffractometry (XRD). The analysis was performed on samples obtained from the specimens used for DPT (which had been desalinated). The XRD samples were prepared by grinding material from the first 5 mm from the surface through which evaporation of the salt solution occurred (corresponding to the treated surface in the case of the consolidated samples). XRD investigation was performed using a PANalytical X’Pert PRO powder diffractometer equipped with a fast X’Celerator detector. CuKα

radiation was used (40 mA, 40 kV). The 2θ range was investigated from 3° to 60° with a step size of 0.1° and time/step of 100 s. Data were processed with HighScore Plus software package (PANalytical).

The amount of sulfate ions (SO_4^{2-}) present in the specimens after the salt crystallization cycles, before and after desalination by poulticing, was determined by ion chromatography (IC), using a Dionex ICS 1000 instrument. The sample to be analyzed by IC (~1 g) was obtained from the specimens and pulverized, then put in deionized water and brought to the boiling point. The saline solution was then obtained by filtering and finally analyzed by IC.

3. RESULTS AND DISCUSSION

3.1. Specimen pre-contamination

To produce the "S-UT" specimens starting from the "UT" specimens, pre-contamination cycles were carried out. The progressive variations in weight and $E_{d\perp}$ of the "S-UT" samples as function of the pre-contamination cycles are illustrated in Figure 2. As expected, the specimens exhibited an initial increase in weight and $E_{d\perp}$, because salts initially filled the pores. Then, when the growing crystals started to exert stress against the pore walls, sample cracking and pulverization occurred, resulting in progressive weight loss and $E_{d\perp}$ decrease. After 6 salt crystallization cycles, the $E_{d\perp}$ of the "S-UT" specimens was decreased by 15% compared to the initial "UT" condition. At this point, the weathering cycles were stopped, not to induce excessive damage that would make it difficult to assess the consolidating effectiveness of the two products.

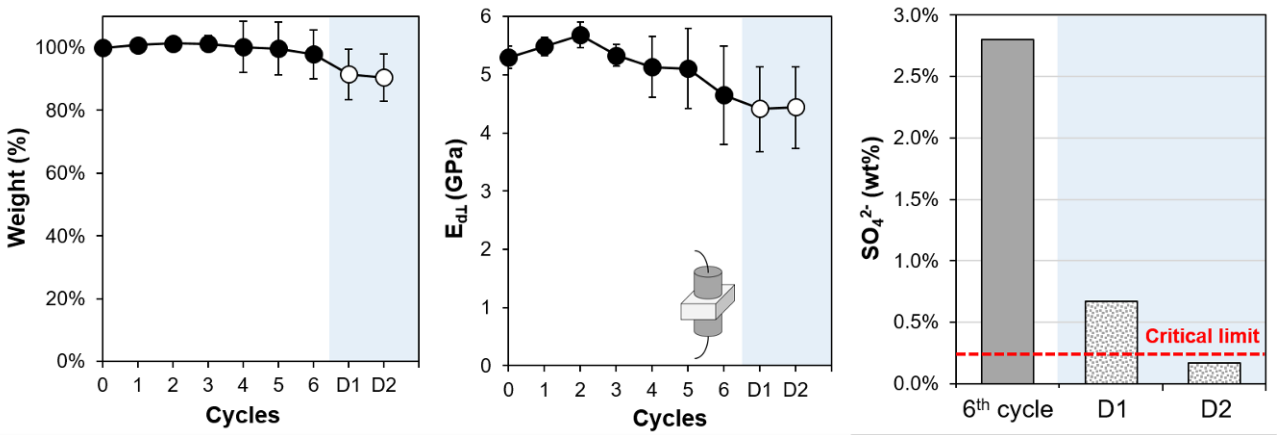

Figure 2. Variations in weight and dynamic elastic modulus in the perpendicular direction ($E_{d\perp}$) and sulfate content after the pre-contamination cycles and desalination repeated twice ("D1" and "D2", blue shading). The critical limit of sulfate content (0.25 wt%) that has been pointed out in the literature [38] as the threshold over which salt removal is recommended is indicated.

To reproduce the conditions that would be experienced in the field in the case of a slightly contaminated mortar or a highly contaminated mortar after salt extraction, the specimens were desalinated by applying a poultice of cellulose pulp. Poulticing, repeated twice, allowed for a significant reduction in the amount of sulfates present in the mortar, from 2.8 wt% to 0.2 wt% (Figure 2). When this latter value was reached, poulticing was stopped, as the amount of residual sulfates was below the value identified in the literature as the critical threshold over which salt extraction is necessary [38], while below this threshold the salt content may be tolerable.

As illustrated in Figure 3 (comparing solid gray bars and dotted gray bars), after pre-contamination and desalination a decreased in $E_{d\perp}$, but not $E_{d//}$, was registered. This was likely due to salt crystallization resulting in the formation of microcracks parallel to the evaporation surface, which significantly affected the $E_{d\perp}$ measurement (because the ultrasonic pulse has to cross the whole specimen thickness, also including the new microcracks), while $E_{d//}$ measurement was not affected (because the ultrasonic pulse can travel parallel to the microcracks). Consistent with the formation of microcracks suggested by the $E_{d\perp}$ reduction, a significant decrease in compressive strength was registered after salt weathering and desalination (Figure 3).

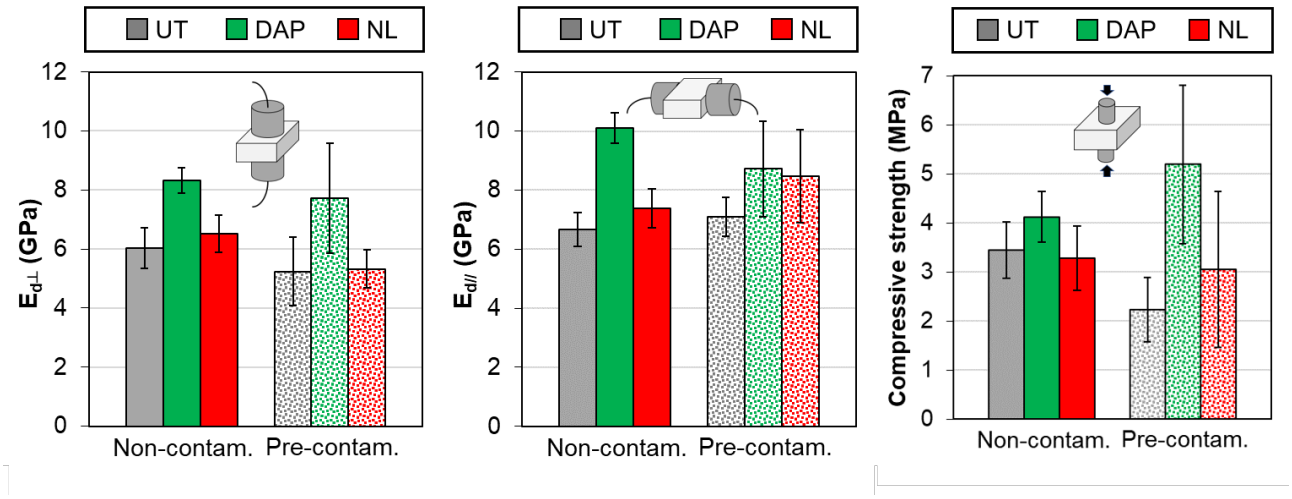

Figure 3. Effects of salt pre-contamination (solid bars vs dashed bars) and consolidation (colored bars vs gray bars), in terms of dynamic elastic modulus in the perpendicular direction ($E_{d\perp}$) and parallel direction ($E_{d//}$) and compressive strength by double punch test (DPT). Values are averages for at least 3 replicates.

The formation of new microcracks after pre-contamination was confirmed by MIP results (Figure 4), which highlighted some increase in the total open porosity and a clear alteration in the pore size distribution, especially in the range between 0.1 and 1 μm, passing from bimodal to unimodal distribution. Tests on untreated samples, before and after salt contamination, were also used to evaluate the reproducibility of the MIP results: while the two samples analyzed in the non-contaminated condition showed almost perfect overlapping, the pre-contaminated samples showed a higher variability (as also registered in terms of weight and E_d changes, Figure 2), as a consequence of salt-induced microcracking.

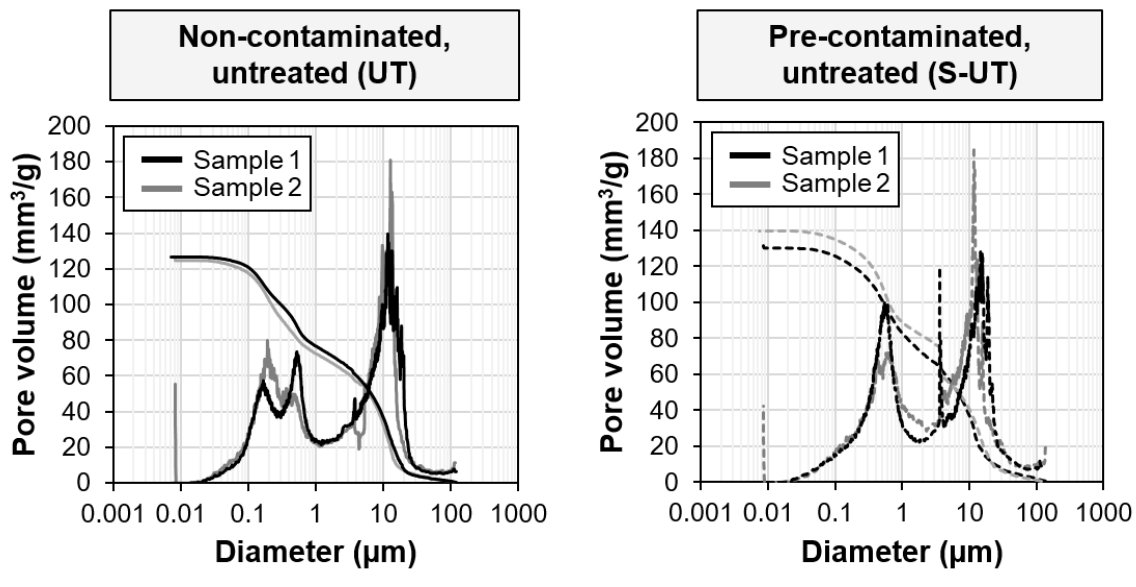

Figure 4. Pore size distribution of non-contaminated and pre-contaminated samples, expressed as cumulative and derivative curves (two samples were tested for each condition).

The results of XRD performed on non-contaminated and pre-contaminated samples are reported in Figure 5. In the untreated reference ("UT"), calcite is the predominant crystalline phase (ICDD 01-085-1108) originated from slaked lime carbonation and originally present in the calcareous aggregate. Furthermore aragonite (ICSD 98-016-9892) and dolomite (ICDD 01-075-1763), originally present in the calcareous aggregate, and portlandite (ICDD 044-1481), due to the residual presence of some non-carbonated slaked lime, were detected. In the pre-contaminated sample ("S-UT"), in addition to the same phases as above, gypsum (ICDD 033-0311) was the only new phase detected, while neither thenardite nor mirabilite were found. This can be explained considering that the analyzed samples had been desalinated to remove soluble salts that may alter mechanical testing and MIP analyses. The formation of gypsum was most likely due to the presence of some residual portlandite when the salt test was performed. Being more water soluble than calcite, portlandite provided Ca^{2+} ions that reacted with SO_4^{2-} ions to form gypsum. In turn, when the samples were desalinated, gypsum (being less soluble that thenardite and mirabilite) was not removed, unlike the other two phases. The fact that portlandite was the origin of gypsum formation is confirmed by the decrease in the intensity of the portlandite peak in the "S-UT" sample, compared to the "UT" one (Figure 5).

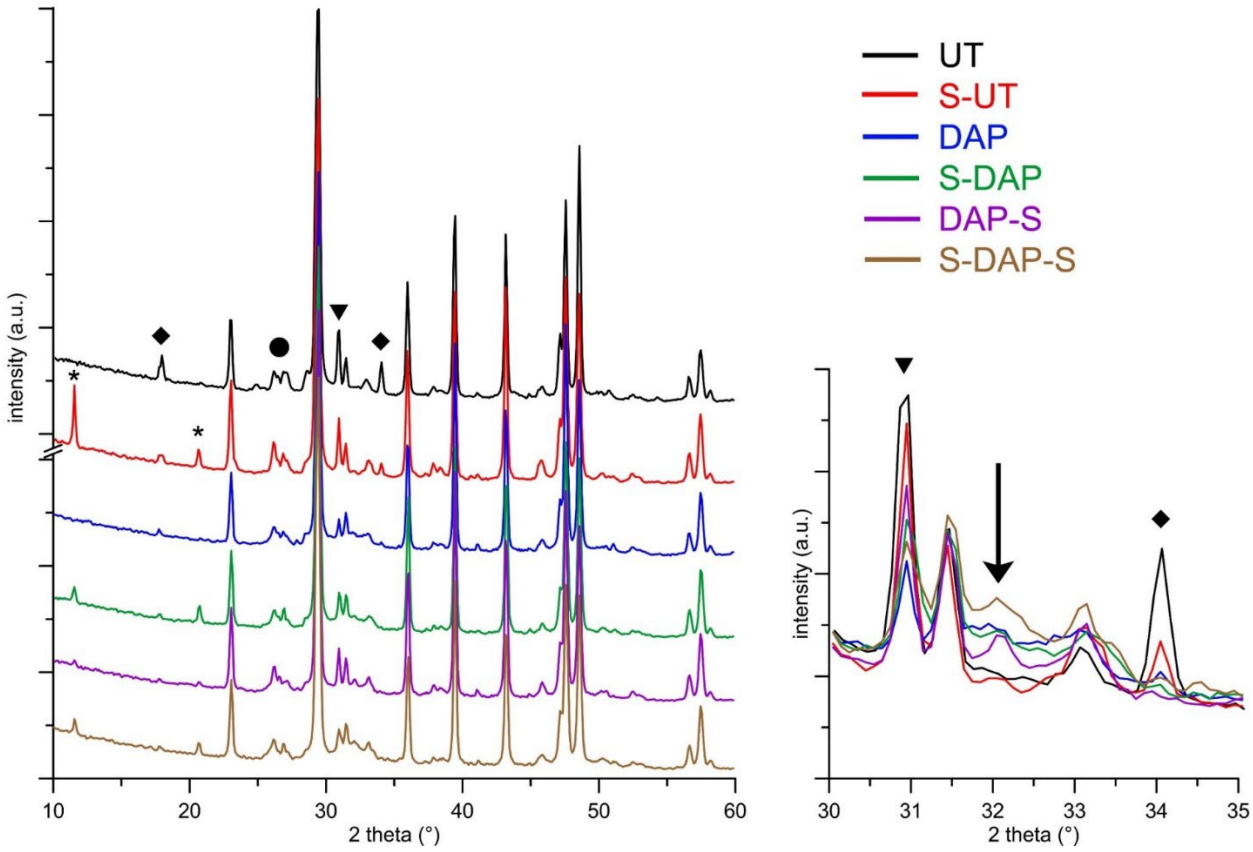

Figure 5. Mineralogical composition of the untreated reference ("UT"), pre-contaminated ("S-UT") and DAP-treated samples ("DAP", "S-DAP", "DAP-S" and "S-DAP-S"). Symbols indicate: (♦) portlandite; (▼) dolomite; (●) aragonite; (*) gypsum. In the magnification on the right, the arrow indicates the broad diffraction signal due to the presence of poorly crystalline carbonate hydroxyapatite.

The SEM observation of the pre-contaminated sample ("S-UT") revealed the presence of some needle-like crystals (Figure 6), which were absent in the "UT" sample and are residues remaining after the desalination step.

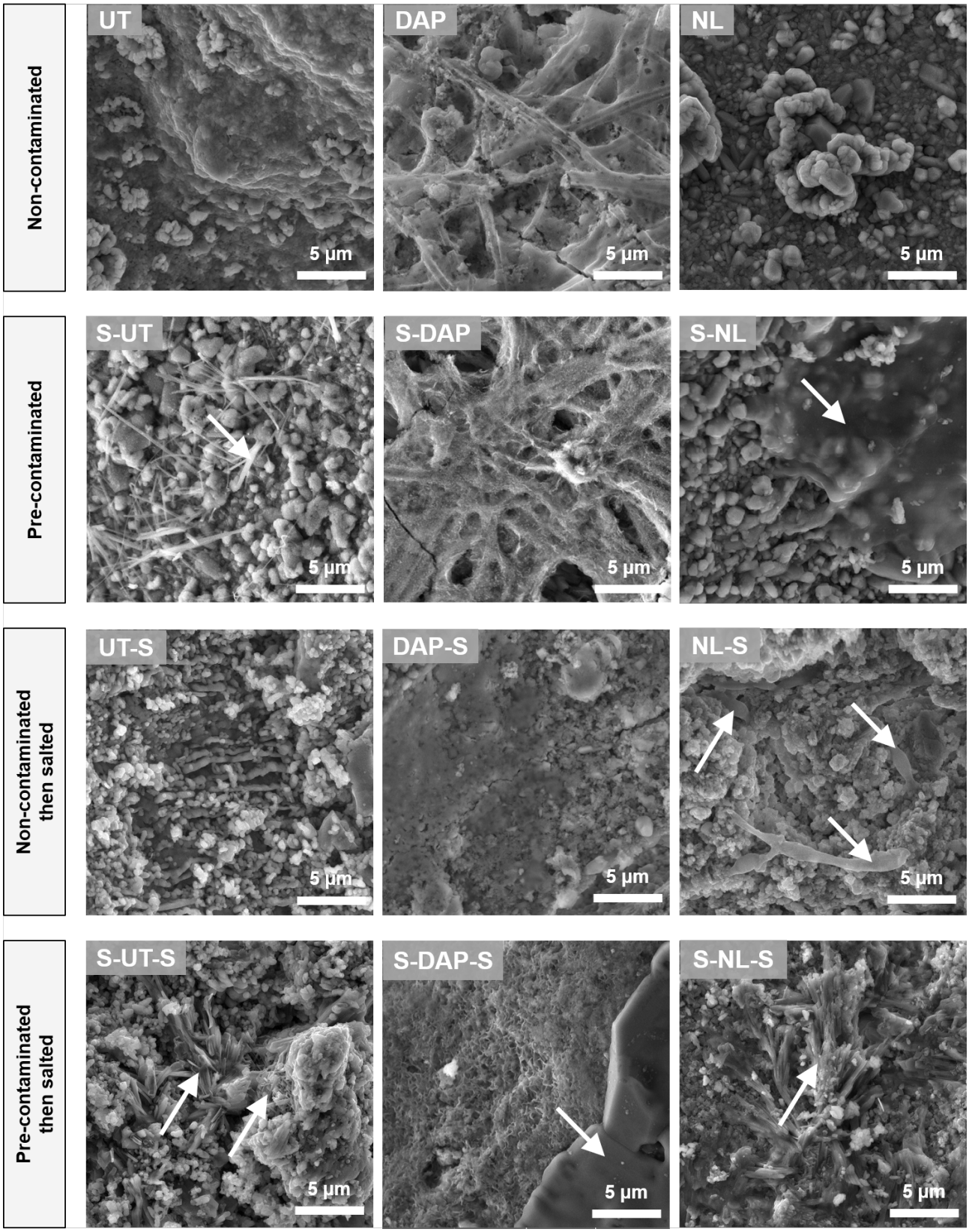

Figure 6. Surface morphology of untreated and treated samples (the analyzed surface was the treated face in consolidated samples and the face through which evaporation took place in salt weathered samples). White arrows indicate new phases formed after salt contamination.

3.2. Consolidating ability

3.2.1 Non-contaminated specimens

The uptake of the liquid consolidant was quite different for the two treatments (4.2 kg/m^2 for DAP and 2.1 kg/m^2 for NL), but the final dry residue of the hardened consolidants was similar (0.2 kg/m^2 for both DAP and NL). Nonetheless, the strengthening effect of the DAP treatment was significantly higher than that of NL (Figure 3), consistently with previous results obtained on lime-based mortars [28,29]. For both consolidants, the E_d increase was higher in the parallel direction, compared to the perpendicular one. This trend is in agreement with previous results obtained on marble specimens [46] and can be attributed to the penetration depth of the consolidants. In fact, the ultrasonic pulse travels through the densest path available. In the parallel direction, this densest path corresponds to the consolidated layer, virtually independently of its thickness. In the perpendicular direction, instead, the ultrasonic pulse has to travel through the whole specimen thickness, so the depth of the consolidated layer influences the measured time to a high extent. In agreement with previous results [46], the increase in E_d caused by DAP is higher than that of NL not only in the parallel direction, but also in the perpendicular one, which suggests a higher penetration depth for the phosphate consolidant.

The strengthening effect detected by UPV in the DAP-treated specimens was confirmed by double punch test (DPT), as the resulting compressive strength was increased by +20% (Figure 3). On the contrary, in the case of NL no substantial improvement was detected by DPT, which is likely due to the consolidant accumulation near the surface, so that no significant increase in bulk mechanical properties could be achieved. This is in agreement with previous results on mortar consolidation, as nanolimes were found to provide a limited increase in the resistance to material loss by scotch tape test, because of consolidant accumulation near the surface [29]. As reported in the literature [47], nanolime accumulation near the treated surface is likely to be ascribed not to poor penetration during the consolidant application, but to back migration of the nanoparticles towards the surface during drying. To maximize in-depth consolidation by NL, different strategies have been proposed (e.g. use of different solvents and sonication of the nano-dispersion before application [47,48]), but in the present study the commercial nanolime consolidant was applied according to the recommendation by the manufacturer (where preliminary sonication is not mentioned).

A sensibly different effect of the two consolidants was found in terms of alterations in the pore system, as assessed by MIP (Figure 7). Compared to the untreated reference, the NL treatment shows minor alterations, namely some occlusion of pores with diameter around 0.2 μm, while the total open porosity remained basically unaltered. Differently, the DAP treatment caused a decrease in the total open porosity and more pronounced alterations in the pore size distribution: the formation of new calcium phosphates in pores with diameter between 0.1 and 1 μm caused partial occlusion of these pores, resulting in an increase in pores with diameter around 0.04 μm. This shift of the pore

size distribution towards smaller pores is important, because the crystallization pressure of salts is known to be higher in smaller pores [1]. Therefore, such alteration in pore size distribution might result in increased crystallization pressure and decreased durability in the long term, hence this aspect should be carefully considered. However, it is important to notice that, in previous studies, a somewhat similar alteration in pore size distribution after consolidation with DAP had been found in limestones [12,23] and mortars [29], but the increases in mechanical properties after consolidation were able to compensate for the unfavorable alteration in pore size distribution, so that the final durability to salt crystallization cycles [12] and freezing-thawing cycles [29] was actually increased, compared to the untreated references.

Based on XRD results (Figure 5), the new consolidating phase formed in the DAP sample is composed of carbonate hydroxyapatite (ICSD 98-015-0309), while there is no evidence of the formation of other calcium phosphate phases (such as octacalcium phosphate or brushite). Formation of carbonate-substituted hydroxyapatite is not surprising, as carbonate ions may be provided by the substrate and by atmospheric CO_2. This result is consistent with previous findings obtained on calcitic powders [49] and calcitic marble [50].

3.2.2 Pre-contaminated specimens

When the consolidants were applied onto pre-contaminated specimens, changes in E_d substantially similar to those observed on non-contaminated specimens were registered (Figure 3), the increase caused by DAP being always higher than that caused by NL. Notable differences were found by DPT, instead (Figure 3).

After pre-contamination by salts, the untreated reference exhibited a significant decrease in compressive strength, as the result of salt-induced damage. After consolidation, NL samples experienced some strength increase, suggesting that the consolidant was able to provide some increase in cohesion. In the case of DAP, the increase in compressive strength achieved on pre-contaminated samples was even higher than on fresh samples (Figure 3). Although counterintuitive, this finding is actually in agreement with previous results reported in the literature when salt-contaminated stone was consolidated with ammonium phosphate [9,18,51] or ammonium oxalate [16,17] solutions. In previous research on ammonium oxalate [17], the higher amount of new consolidating phases found in the case of salt-containing stone was attributed to the different surface texture and the greater surface area available to react with the consolidating solutions, compared to the condition when no salts are present. A similar mechanism could be responsible for the higher consolidating efficacy registered in the present study in the case of pre-contaminated samples, although specific additional tests would be necessary to verify this hypothesis.

The alteration in pore size distribution owing to the two consolidants was substantially similar to that registered in the non-contaminate samples (Figure 7). Starting from the salt-contaminated reference condition ("S-UT"), the "S-NL" showed minor differences, while the "S-DAP" sample showed an increase in pores with diameter around 0.05 μm similar to that of the "DAP" sample.

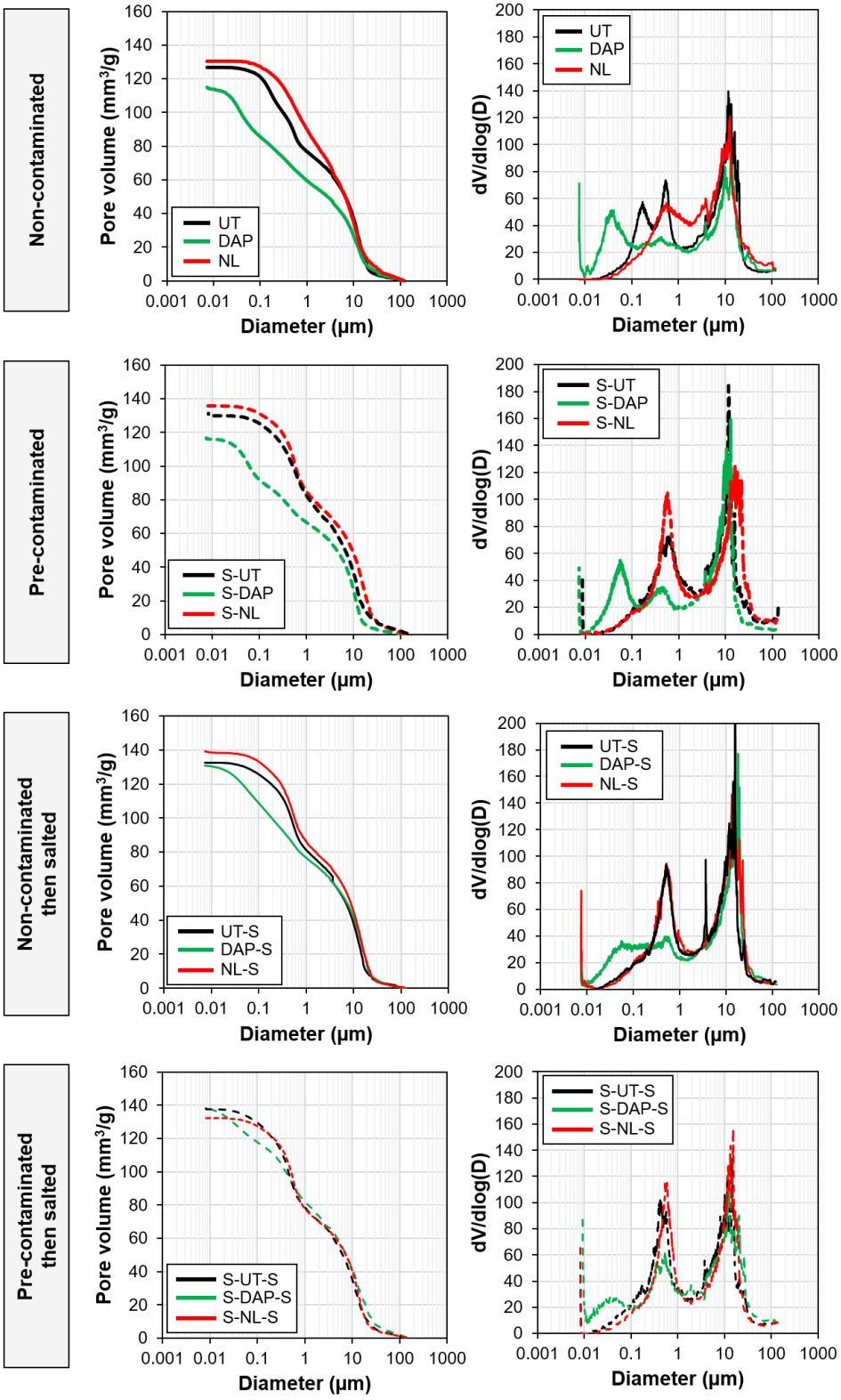

Figure 7. Pore size distributions of non-contaminated (solid lines) and pre-contaminated (dashed lines) samples, expressed as cumulative (left) and derivative curves (right).

In the “S-DAP” sample, XRD detected both gypsum (owing to salt pre-contamination) and poorly crystalline carbonate hydroxyapatite (owing to the consolidating treatment) (Figure 5). Morphologies attributed to these two phases were clearly visible by SEM on the sample surface (Figure 8). Notably, no clear evidence of Na-substituted hydroxyapatite was found by XRD (Figure 5). This finding is important because it indicates that, at least in the investigated conditions (SO_4^{2-} = 0.2 wt%), contamination with sodium sulfate proved not to negatively affect the DAP treatment. This was not obvious, considering that: (i) the presence of sodium ions in the surrounding aqueous solution has been reported to inhibit the formation of hydroxyapatite (HAP) [31]; (ii) in case sodium ions are incorporated into the HAP crystal structure, the resulting sodium-substituted HAP is energetically less stable compared to HAP, resulting in higher dissolution [52]. The formation of carbonate hydroxyapatite, with no apparent interference from sodium contamination, can hence be considered a positive result.

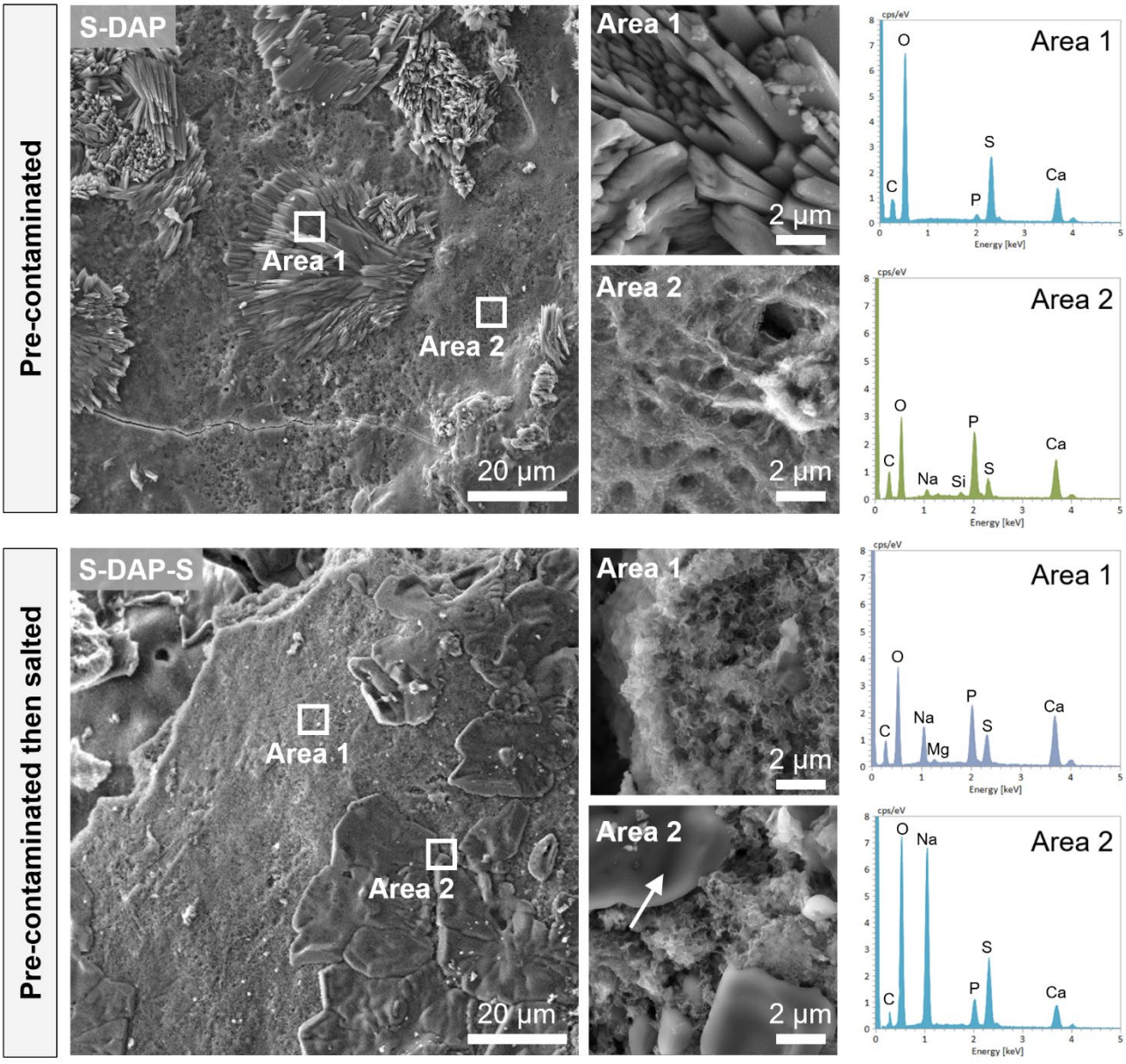

Figure 8. Surface morphology and EDS spectra of “S-DAP” and “S-DAP-S” samples (after desalination).

3.3. Resistance to salt weathering after consolidation

3.3.1 Non-contaminated specimens

The E_d evolution in the two directions and the weight change as a function of the salt crystallization cycles are illustrated in Figure 9, together with the final values after desalination.

Initially, all the specimens exhibited an apparent increase in E_d and weight, owing to pore filling by salts. Given the higher consolidating ability of the DAP treatment, the DAP samples showed the highest E_d in both directions until the 5th cycle, when a sudden drop was experienced, especially in the perpendicular direction. This was most likely due to the formation of cracks parallel to the specimen surface through which the salt solution evaporated. While the $E_{d\perp}$ (measured perpendicular to this surface) was highly affected, $E_{d//}$ was impacted to a lower extent. From the 6th to the 7th cycle, a further big drop in $E_{d\perp}$ (but not $E_{d//}$) was registered, together with a significant weight loss, owing to the salt-induced detachment of scales roughly parallel to the evaporation surface. When salt weathering was stopped after 10 cycles and the specimens were desalinated, an apparent increase in $E_{d\perp}$ was experienced. This can be explained considering that, when the salts were removed from the cracks, the mortar parts could get closer together and the mortar cohesion apparently increased. After desalination, all the conditions exhibited similar $E_{d//}$, while DAP apparently showed a higher decrease in weight and $E_{d\perp}$. This can be attributed to the alterations in pore size distribution caused by the DAP treatment ("DAP" sample, Figure 7), namely an increase in the amount of pores around 0.04-0.05 μm. Because salt crystallization pressure is higher in smaller pores [1], such an alteration in the pore system is unfavorable. It is noteworthy that, after the salt cycles ("DAP-S" sample, Figure 7), the amount of pores around 0.04-0.05 μm is diminished, probably because of some residual salts remaining even after desalination.

In spite of the unfavorable alteration in pore size distribution, when the residual compressive strength after salt weathering was assessed by DPT, the DAP-treated specimens still exhibited higher residual strength than NL (Figure 9). This is thought to be a consequence of the initial consolidating effect of the DAP treatment: the improvement in mechanical properties was able to compensate for the higher crystallization pressure, so in the end the resistance of DAP-treated mortar is not lower than the untreated reference and actually higher than that of mortar treated with nanolimes.

After consolidation and subsequent salt weathering, different morphologies were observed on the various samples (Figure 6). In the case of the "DAP-S" sample, XRD detected carbonate hydroxyapatite and gypsum (Figure 5), consistently with results discussed above.

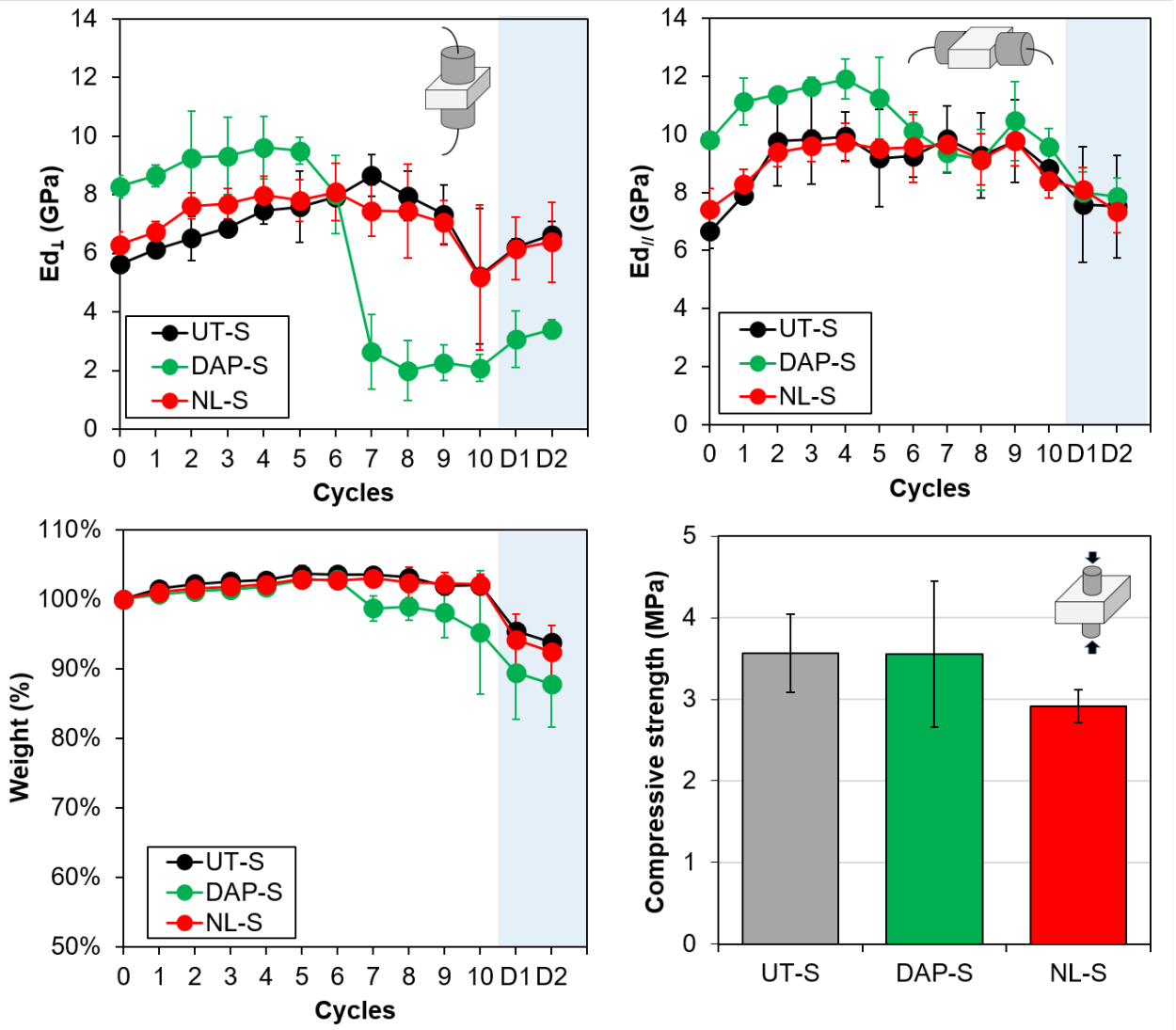

Figure 9. Effects of salt crystallization cycles on samples initially non-contaminated, in terms of dynamic elastic modulus in the perpendicular direction ($E_d\perp$) and parallel direction (E_d//), weight and compressive strength by DPT. The blue shading indicates desalination repeated twice ("D1" and "D2"). The different starting points of each condition depends on the different consolidating ability. Values are averages for at least 3 replicates.

3.3.2 Pre-contaminated specimens

The E_d evolution in the two directions and weight change as a function of the salt crystallization cycles are illustrated in Figure 10, where the final compressive strength by DPT is also reported.

In this case, the evolution in E_d and weight was substantially similar for the three conditions, with differences in the residual weight appearing only after desalination at the end of the cycles. In these conditions, the DAP samples apparently experienced lower material loss. In a similar way as already found for pre-contaminated samples right after consolidation (Figure 3), also after additional salt weathering cycles the DAP samples exhibited the highest residual compressive strength at the end of the cycles (Figure 10). This is notable and confirms that the improvement in mechanical properties after consolidation is able to compensate for the unfavorable alteration in pore size distribution after

treatment (Figure 7), thus finally leading to higher residual strength than both the untreated reference and the alternative consolidant. Regarding the NL samples, similar to the situation right after consolidation (Figure 3), also after additional salt weathering they exhibited some benefit compared to the untreated mortar, although less than DAP (Figure 10).

After the salt cycles and desalination, XRD revealed the same phases also found in the case of the initially non-contaminated samples (gypsum and carbonate hydroxyapatite, Figure 5). Notably, also in this case no clear evidence of the formation of Na-substituted HAP was found.

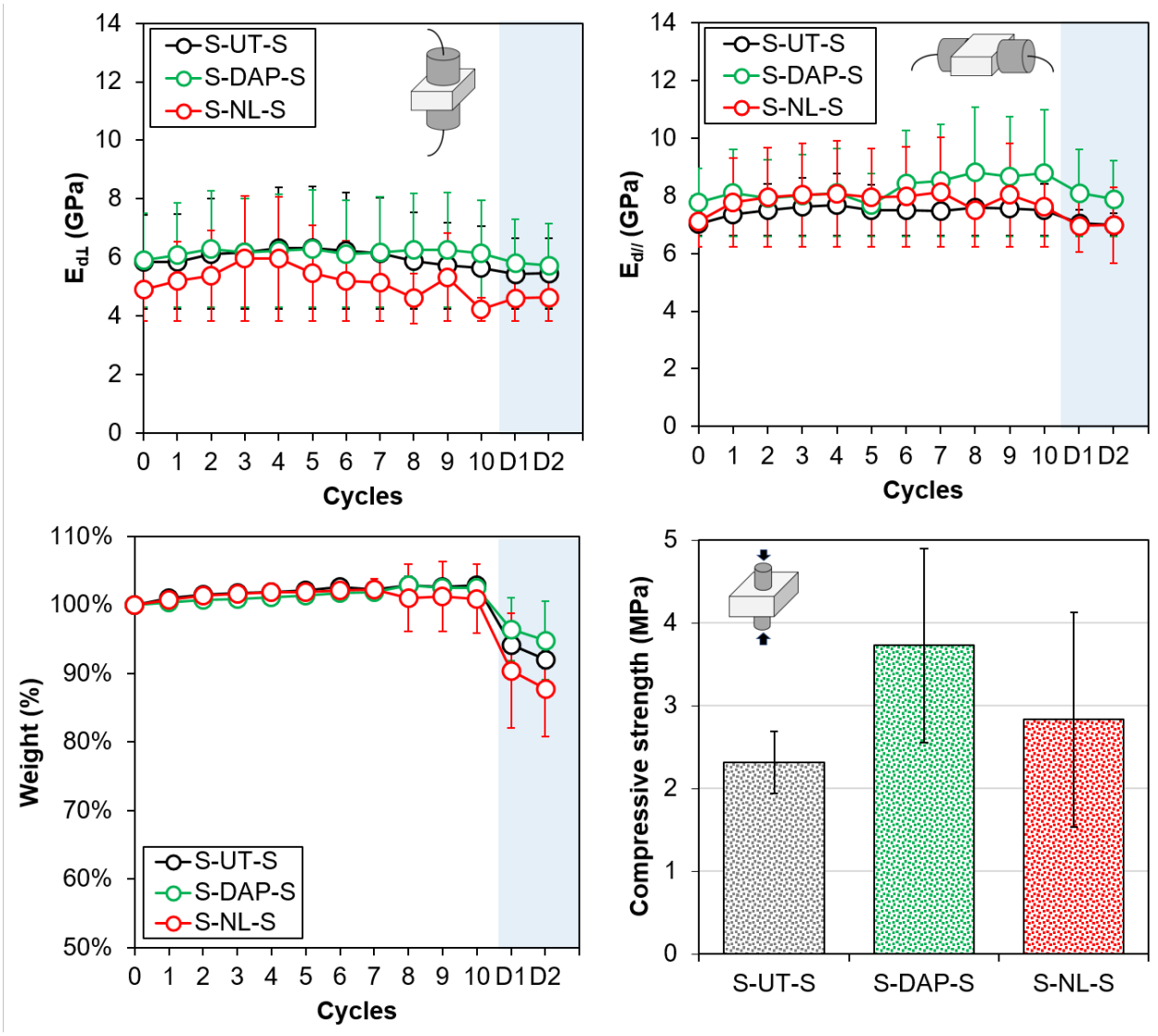

Figure 10. Effects of salt crystallization cycles on samples initially pre-contaminated, in terms of dynamic elastic modulus in the perpendicular direction ($E_{d\perp}$) and parallel direction ($E_{d//}$), weight and compressive strength by DPT. The blue shading indicates desalination repeated twice ("D1" and "D2"). The different starting points of each condition depends on the different consolidating ability. Values are averages for at least 3 replicates.

4. CONCLUSIONS

The present study aimed at evaluating the influence of salt contamination on the consolidating effectiveness and durability to further salt weathering of two inorganic products, namely ammonium phosphate (DAP) and nanolimes (NL). The consolidants were applied onto slaked lime-based mortars that were subjected to salt weathering by sodium sulfate before and/or after consolidation. Based on the obtained results, the following conclusions can be drawn:

1) The consolidating ability of the DAP treatment proved to be higher than that of NL, both on non-contaminated and pre-contaminated specimens, as assessed by ultrasounds and double punch test to determine the specimen compressive strength.
2) The initial presence of salts inside the mortar pores did not negatively affect the performance of the consolidants. On the contrary, the consolidating effectiveness of DAP resulted actually increased (consistently with previous results [9,51]), likely because the salts increased the surface area, thus favoring formation of the new calcium phosphate phases.
3) In the case of the DAP treatment, carbonate hydroxyapatite was formed as the new consolidating phase in both the non-contaminated and pre-contaminated specimens. The initial presence of sodium sulfate inside the mortar pores did not negatively affect the DAP treatment. This is notable, because sodium is known to inhibit formation of hydroxyapatite [31] and to decrease its stability in case Na-substituted hydroxyapatite is formed [52]. Therefore, it is important to be able to exclude that either mechanism took place.
4) The DAP treatment caused a significant alteration in the pore size distribution of the mortar, namely partial occlusion of pores with diameter between 0.1 and 1 μm and an increase in pores with diameter around 0.04 μm. This shift of the pore size distribution towards smaller pores is unfavorable, because the crystallization pressure of salts is known to be higher in smaller pores [1].
5) Notwithstanding the unfavorable alteration in pore size distribution, the improvement in mechanical properties caused by the DAP treatment was able to compensate for the increased crystallization pressure. In fact, when additional salt crystallization cycles were performed after consolidation, the final compressive strength of the DAP-samples was fully comparable or higher than that of the untreated reference, in all cases resulting higher than the NL-samples.

All things considered, the presence of sodium sulfate (at least in the investigated conditions, i.e. SO_4^{2-} = 0.2 wt%) in the mortar pores proved to have no negative effect on the performance of the DAP-based treatment. This finding is in agreement with previous results on the performance of the DAP treatment on marble contaminated with sodium chloride [51] and limestone contaminated with sodium sulfate [9]. This is important to ensure a successful performance of this innovative consolidant in the practice of monument conservation in the field, where the substrates are often contaminated with salts.

When evaluating the performance of both consolidants in terms of resistance to salt weathering after consolidation, it should be noted that the adopted salt weathering test (involving the high $Na_2SO_4 \cdot 10H_2O$ concentration recommended in the European Standard 12370 [36]) has been criticized in the past for being too aggressive. As a result of such high aggressiveness, the benefits provided by the two consolidants compared to the untreated reference might have been flattened. In fact, the salt weathering test might induce very high stress that none of the consolidants is able to resist effectively, even though such high stress might actually never be experienced in the field. A strong impact of the salt weathering test adopted in this study is also suggested by the fact that, in a previous study on the durability to freezing-thawing cycles, DAP-consolidated mortars exhibited significantly better durability than NL-treated ones [29], thus showing a different trend than what assessed in the present study. Therefore, future research will be dedicated to evaluating the durability of consolidated mortars subjected to milder and more reliable salt weathering tests, such as that being developed within the RILEM TC 271-ASC [35,53].

REFERENCES

[1] G. W. Scherer, “Crystallization in pores,” *Cem. Concr. Res.*, vol. 29, no. 8, pp. 1347–1358, 1999, doi: 10.1016/S0008-8846(99)00002-2.

[2] E. Dohene and Price Clifford A., *Research in Conservation*, no. 2. 2010.

[3] R. Nogueira, A. P. Ferreira Pinto, and A. Gomes, “Artificial ageing by salt crystallization: test protocol and salt distribution patterns in lime-based rendering mortars,” *J. Cult. Herit.*, vol. 45, pp. 180–192, 2020, doi: 10.1016/j.culher.2020.01.013.

[4] S. J. C. Granneman, B. Lubelli, and R. P. J. van Hees, “Mitigating salt damage in building materials by the use of crystallization modifiers – a review and outlook,” *J. Cult. Herit.*, vol. 40, pp. 183–194, 2019, doi: 10.1016/j.culher.2019.05.004.

[5] M. Bassi, E. Sassoni, and E. Franzoni, “Experimental Study on an Innovative Biopolymeric Treatment Against Salt Deterioration of Materials in Cultural Heritage,” *Front. Mater.*, vol. 8, no. February, pp. 1–22, 2021, doi: 10.3389/fmats.2021.583112.

[6] V. Vergès-Belmin, A. Heritage, and A. Bourgès, Powdered Cellulose Poultices in Stone and Wall Painting Conservation: Myths And Realities, Studies in Conservation , 2011, Vol. 56, No. 4 (2011), pp. 281-297, doi: 10.1179/204705811X13159282692923.

[7] G. W. Scherer and G. S. Wheeler, “Silicate consolidants for stone,” *Key Eng. Mater.*, vol. 391, pp. 1–25, 2009, doi: 10.4028/www.scientific.net/kem.391.1.

[8] S. A. Ruffolo *et al.*, “New insights on the consolidation of salt weathered limestone: the case study of Modica stone,” *Bull. Eng. Geol. Environ.*, vol. 76, no. 1, pp. 11–20, 2017, doi: 10.1007/s10064-015-0782-1.

[9] G. Graziani, E. Sassoni, G. W. Scherer, and E. Franzoni, “Phosphate-based treatments for consolidation of salt-bearing Globigerina limestone,” *IOP Conf. Ser. Mater. Sci. Eng.*, vol. 364, no. 1, 2018, doi: 10.1088/1757-899X/364/1/012082.

[10] G. Wheeler, *Alkoxysilanes and the Consolidation of Stone*, vol. 46, no. 2. 2005.

[11] A. Moropoulou, G. Haralampopoulos, T. Tsiourva, F. Auger, and J. M. Birginie, “Artificial

weathering and non-destructive tests for the performance evaluation of consolidation materials applied on porous stones," *Mater. Struct. Constr.*, vol. 36, no. 258, pp. 210–217, 2003, doi: 10.1617/13773.

[12] E. Sassoni, G. Graziani, and E. Franzoni, "An innovative phosphate-based consolidant for limestone. Part 2: Durability in comparison with ethyl silicate," *Constr. Build. Mater.*, vol. 102, pp. 931–942, 2016, doi: 10.1016/j.conbuildmat.2015.10.202.

[13] E. Molina, C. Fiol, and G. Cultrone, "Assessment of the efficacy of ethyl silicate and dibasic ammonium phosphate consolidants in improving the durability of two building sandstones from Andalusia (Spain)," *Environ. Earth Sci.*, vol. 77, no. 8, pp. 1–15, 2018, doi: 10.1007/s12665-018-7491-6.

[14] S. A. Ruffolo *et al.*, "Efficacy of nanolime in restoration procedures of salt weathered limestone rock," *Appl. Phys. A Mater. Sci. Process.*, vol. 114, no. 3, pp. 753–758, 2014, doi: 10.1007/s00339-013-7982-y.

[15] D. Pinna, B. Salvadori, and S. Porcinai, "Evaluation of the application conditions of artificial protection treatments on salt-laden limestones and marble," *Constr. Build. Mater.*, vol. 25, no. 5, pp. 2723–2732, 2011, doi: 10.1016/j.conbuildmat.2010.12.023.

[16] T. Dreyfuss, "Interactions on site between powdering porous limestone, natural salt mixtures and applied ammonium oxalate," *Herit. Sci.*, vol. 7, no. 1, pp. 1–8, 2019, doi: 10.1186/s40494-019-0247-0.

[17] T. Mifsud and J. Cassar, "The treatment of weathered Globigerina Limestone: The surface conversion of calcium carbonate to calcium oxalate," *Proc. Int. Conf. Heritage, Weather. Conserv. HWC 2006*, vol. 2, pp. 727–734, 2006.

[18] E. Sassoni, G. Graziani, and E. Franzoni, "Repair of sugaring marble by ammonium phosphate: Comparison with ethyl silicate and ammonium oxalate and pilot application to historic artifact," Mater. Des., vol. 88, pp. 1145–1157, 2015, doi: 10.1016/j.matdes.2015.09.101.

[19] A. Shekofteh, E. Molina, L. Rueda-Quero, A. Arizzi, and G. Cultrone, "The efficiency of nanolime and dibasic ammonium phosphate in the consolidation of beige limestone from the Pasargadae World Heritage Site," *Archaeol. Anthropol. Sci.*, vol. 11, no. 9, pp. 5065–5080, 2019, doi: 10.1007/s12520-019-00863-y.

[20] E. Molina, L. Rueda-Quero, D. Benavente, A. Burgos-Cara, E. Ruiz-Agudo, and G. Cultrone, "Gypsum crust as a source of calcium for the consolidation of carbonate stones using a calcium phosphate-based consolidant," *Constr. Build. Mater.*, vol. 143, pp. 298–311, 2017, doi: 10.1016/j.conbuildmat.2017.03.155.

[21] E. Sassoni, C. Mazzotti, and G. Pagliai, "Comparison between experimental methods for evaluating the compressive strength of existing masonry buildings", *Constr. Build. Mater.*, vol. 68, pp. 206-219, 2014, doi:10.1016/j.conbuildmat.2014.06.070.

[22] F. Pino, et al., "Advanced mortar coatings for cultural heritage protection. Durability towards prolonged UV and outdoor exposure", Environmental Science and Pollution Research, Vol. 24, pp. 12608-12617, 2017, doi: 10.1007/s11356-016-7611-3.

[23] E. Sassoni, S. Naidu, and G. W. Scherer, "The use of hydroxyapatite as a new inorganic consolidant for damaged carbonate stones," *J. Cult. Herit.*, vol. 12, no. 4, pp. 346–355, 2011, doi: 10.1016/j.culher.2011.02.005.

[24] G. Graziani, E. Sassoni, G. W. Scherer, and E. Franzoni, "Resistance to simulated rain of hydroxyapatite- and calcium oxalate-based coatings for protection of marble against corrosion," *Corros. Sci.*, vol. 127, no. August, pp. 168–174, 2017, doi: 10.1016/j.corsci.2017.08.020.

[25] E. Sassoni, G. Graziani, E. Franzoni, and G. W. Scherer, “Calcium phosphate coatings for marble conservation: Influence of ethanol and isopropanol addition to the precipitation medium on the coating microstructure and performance,” *Corros. Sci.*, vol. 136, pp. 255–267, 2018, doi: 10.1016/j.corsci.2018.03.019.

[26] E. Sassoni and E. Franzoni, “Lime and cement mortar consolidation by ammonium phosphate,” *Constr. Build. Mater.*, vol. 245, p. 118409, 2020, doi: 10.1016/j.conbuildmat.2020.118409.

[27] A. Defus *et al.*, “Di-ammonium hydrogen phosphate for the consolidation of lime-based historic mortars – Preliminary research,” *J. Cult. Herit.*, vol. 48, no. February, pp. 45–53, 2021, doi: 10.1016/j.culher.2021.01.005.

[28] G. Masi and E. Sassoni, “Comparison between ammonium phosphate and nanolimes for render consolidation,” *IOP Conf. Ser. Mater. Sci. Eng.*, vol. 949, no. 1, 2020, doi: 10.1088/1757-899X/949/1/012039.

[29] G. Masi and E. Sassoni, “Air lime mortar consolidation by nanolimes and ammonium phosphate: Compatibility, effectiveness and durability,” *Constr. Build. Mater.*, vol. 299, p. 123999, 2021, doi: 10.1016/j.conbuildmat.2021.123999.

[30] A. Bigi, E. Boanini, M. Gazzano, "Ion substitution in biological and synthetic apatites". In Biomineralization and Biomaterials: Fundamentals and Applications; Aparicio, C., Ginebra, M.P., Eds.; Woodhead Publishing (Elsevier): Sawston, UK, 2016; pp. 235–266. doi: 10.1016/B978-1-78242-338-6.00008-9

[31] A. Ressler, A. Žužić, I. Ivanišević, N. Kamboj, and H. Ivanković, “Ionic substituted hydroxyapatite for bone regeneration applications: A review,” *Open Ceram.*, vol. 6, no. May, 2021, doi: 10.1016/j.oceram.2021.100122.

[32] C. Rodriguez-Navarro and E. Ruiz-Agudo, “Nanolimes: From synthesis to application,” *Pure Appl. Chem.*, vol. 90, no. 3, pp. 523–550, 2018, doi: 10.1515/pac-2017-0506.

[33] D. Chelazzi, G. Poggi, Y. Jaidar, N. Toccafondi, R. Giorgi, and P. Baglioni, “Hydroxide nanoparticles for cultural heritage: Consolidation and protection of wall paintings and carbonate materials,” *J. Colloid Interface Sci.*, vol. 392, no. 1, pp. 42–49, 2013, doi: 10.1016/j.jcis.2012.09.069.

[34] Various Authors, "Corso sulla manutenzione di dipinti murali - Mosaici - Stucchi, Tecniche di esecuzione e materiali costitutivi", Istituto Centrale per il Restauro, 1986.

[35] B. Lubelli *et al.*, “Towards a more effective and reliable salt crystallization test for porous building materials: state of the art,” *Mater. Struct. Constr.*, vol. 51, no. 2, 2018, doi: 10.1617/s11527-018-1180-5.

[36] European Standard EN 12370, "Natural Stone test methods- Determination of resistance to salt crystallisation", 2020.

[37] D. Benavente, M. A. García Del Cura, A. Bernabéu, and S. Ordóñez, “Quantification of salt weathering in porous stones using an experimental continous partial immersion method,” *Eng. Geol.*, vol. 59, no. 3–4, pp. 313–325, 2001, doi: 10.1016/S0013-7952(01)00020-5.

[38] J. Feijoo, O. Matyščák, L. M. Ottosen, T. Rivas, and X. R. Nóvoa, “Electrokinetic desalination of protruded areas of stone avoiding the direct contact with electrodes,” *Mater. Struct. Constr.*, vol. 50, no. 1, pp. 1–15, 2017, doi: 10.1617/s11527-016-0946-x.

[39] E. Franzoni, E. Sassoni, and G. Graziani, “Brushing, poultice or immersion? The role of the application technique on the performance of a novel hydroxyapatite-based consolidating treatment for limestone,” *J. Cult. Herit.*, vol. 16, no. 2, pp. 173–184, 2015, doi: 10.1016/j.culher.2014.05.009.

[40] G. Graziani, E. Sassoni, G. W. Scherer, and E. Franzoni, “Penetration depth and redistribution of an aqueous ammonium phosphate solution used for porous limestone consolidation by brushing and immersion,” *Constr. Build. Mater.*, vol. 148, pp. 571–578, 2017, doi: 10.1016/j.conbuildmat.2017.05.097.

[41] J. Ruedrich, C. Knell, J. Enseleit, Y. Rieffel, and S. Siegesmund, “Stability assessment of marble statuaries of the Schlossbrücke (Berlin, Germany) based on rock strength measurements and ultrasonic wave velocities,” *Environ. Earth Sci.*, vol. 69, no. 4, pp. 1451–1469, 2013, doi: 10.1007/s12665-013-2246-x.

[42] S. Weiss, T, Rasolofosaon, P. N.L., Siegesmund, “Ultrasonic wave velocities as a diagnostic tool for the quality assessment of marble,” *Nat. stone, Weather. phenomena, Conserv. Strateg. case Stud. Geol. Soc. London*, vol. 205, pp. 149–164, 2022.

[43] A. Arizzi, L. S. Gomez-Villalba, P. Lopez-Arce, G. Cultrone, and R. Fort, “Lime mortar consolidation with nanostructured calcium hydroxide dispersions: the efficacy of different consolidating products for heritage conservation,” *Eur. J. Mineral.*, vol. 27, no. 3, pp. 311–323, 2015, doi: 10.1127/ejm/2015/0027-2437.

[44] J. Henzel, S. Karl, Determination of strength of mortar in the joints of masonry by compression tests on small specimens, Darmstadt Concrete 2 (1987) 123-136

[45] E. Sassoni, E. Franzoni, and C. Mazzotti, “Influence of sample thickness and capping on characterization of bedding mortars from historic masonries by double punch test (DPT),” *Key Eng. Mater.*, vol. 624, no. October, pp. 322–329, 2015, doi: 10.4028/www.scientific.net/KEM.624.322.

[46] E. Sassoni, G. Ugolotti, and M. Pagani, “Nanolime, nanosilica or ammonium phosphate? Laboratory and field study on consolidation of a byzantine marble sarcophagus,” *Constr. Build. Mater.*, vol. 262, p. 120784, 2020, doi: 10.1016/j.conbuildmat.2020.120784.

[47] G. Borsoi, B. Lubelli, R. van Hees, R. Veiga, A. Santos Silva, L. Colla, L. Fedele, P. Tomasin, "Effect of solvent on nanolime transport within limestone: How to improve in-depth deposition", *Colloids and Surfaces A: Physicochem. Eng. Aspects*, vol. 497, pp. 171-181, 2016

[48] G. Borsoi, B. Lubelli, R. van Hees, R. Veiga, A. Santos Silva, "Understanding the transport of nanolime consolidants within Maastricht limestone", *J. Cult. Herit.*, vol. 18, pp. 242-249, 2016

[49] E. Possenti *et al.*, “New insight on the interaction of diammonium hydrogenphosphate conservation treatment with carbonatic substrates: A multi-analytical approach,” *Microchem. J.*, vol. 127, pp. 79–86, 2016, doi: 10.1016/j.microc.2016.02.008.

[50] E. Possenti *et al.*, “Diammonium hydrogenphosphate for the consolidation of building materials. Investigation of newly-formed calcium phosphates,” *Constr. Build. Mater.*, vol. 195, pp. 557–563, 2019, doi: 10.1016/j.conbuildmat.2018.11.077.

[51] G. Ugolotti, G. Masi, E. Sassoni, “Interaction between sodium chloride and ammonium phosphate on carrara marble: two laboratory approaches,” in *Fifth International Conference on salt weathering of buildings and stone sculptures (SWBSS), 22-24 September 2021, The Netherlands*, 2021, pp. 119–128.

[52] J. Sang Cho *et al.*, “Enhanced osteoconductivity of sodium-substituted hydroxyapatite by system instability,” *J. Biomed. Mater. Res. - Part B Appl. Biomater.*, vol. 102, no. 5, pp. 1046–1062, 2014, doi: 10.1002/jbm.b.33087.

[53] R. J. Flatt *et al.*, “Predicting salt damage in practice: a theoretical insight into laboratory tests,” *RILEM Tech. Lett.*, vol. 2, pp. 108–118, 2017, doi: 10.21809/rilemtechlett.2017.41.